Proceedings of ASME Turbo Expo 2011
GT2011
June 6-10, 2011, Vancouver, British Columbia, Canada

GT2011-46221

EXPERIMENTAL AND NUMERICAL INVESTIGATION OF AN AERODYNAMICALLY LOADED GUIDE VANE IN A TURBINE DUCT

Martin Johansson*
Dept. of Applied Mechanics
Chalmers University of Technology
412 96 Gothenburg, Sweden
Email: martin.johansson@chalmers.se

Valery Chernoray
Dept. of Applied Mechanics
Chalmers University of Technology
412 96 Gothenburg, Sweden

Linda Ström
Dept. of Aero and Thermo Dynamics
Volvo Aero Corporation
461 81 Trollhättan, Sweden

Jonas Larsson
Dept. of Aero and Thermo Dynamics
Volvo Aero Corporation
461 81 Trollhättan, Sweden

Hans Abrahamsson
Dept. of Aero and Thermo Dynamics
Volvo Aero Corporation
461 81 Trollhättan, Sweden

ABSTRACT

To obtain validation for an aerodynamically loaded guide vane in a turbine duct, a new configuration was implemented in the large-scale low-speed turbine rig facility at Chalmers University of Technology. The new configuration represents a modern counter rotating turbine design, with a flow turning structural vane.

The flow in a turbine duct is very complex, due to the influence of the upstream turbine stage flow structures, and becomes even more complex if the turbine duct is equipped with an aerodynamically loaded structural vane. The flow has large secondary motions and is sensitive to flow separation, which is difficult to predict with numerical CFD methods. Very limited information is found in the open literature that can be used for validation of numerical methods.

This paper presents the new experimental configuration and validation of its aerodynamic performance. Measurements including surface pressure, mapping of pressure losses and flow structures are presented and discussed. Comparison to initial CFD analyses enhance the understanding of the flow structures and gives a preliminary validation of used methods.

INTRODUCTION

The turbine duct is the part of the gas path that connects the high pressure turbine (HPT) with the downstream intermediate or low pressure turbine (IPT, LPT), and preferably this duct has a large radial offset in order to obtain an efficient IPT/LPT. The turbine duct is usually equipped with a thick aerodynamic guide vane, due to internal clearance requirements for e.g. oil and air supplies to the engine internal domains. Some engines also have a turbine structure in between the HPT and IPT/LPT, which connects the engine outer case to the internal bearings, which require clearance. Depending on the engine system architecture, the guide vane could either be aerodynamically unloaded or loaded, i.e. turning the flow. The objective of the present investigation is to study a low turning structural guide vane, representative for a modern counter rotating engine system design. In a counter rotating system design, the flow in the duct is turned in the same direction as the HPT exit swirl, which then require less turning vs. a co-rotating system design. A counter rotating design enables a more efficient turbine duct design with possibility to increased radial offset and reduced axial length.

The flow field in the turbine duct and around the guide vane is very complex and difficult to predict with CFD. Despite the

*Address all correspondence to this author.

large area ratio of the duct (increase in cross sectional area from the HPT to the IPT/LPT), the flow velocity is preserved through the duct, due to the increased swirl component created by the turning vane. An increase of the radial offset of the duct in combination with the goal of keeping the overall length short, create an S-shaped duct, which increase the risk for flow separation. The combination of an S-shaped duct and a turning guide vane create a complex flow field with secondary flow motions, which could cause high pressure losses or local separation. Furthermore, the flow structures from the upstream HP stage influences the flow in the duct. Most predominant is the blade tip leakage flow, with different flow angle, which cause strong secondary flows and is a pressure loss contributor. The duct inlet flow also shows non-uniformity with flow structures from upstream HP vane, which influences the near wall flow as presented by Arroyo [1]. Hence, there are great demands on the design of a turbine duct with a turning vane. Separation is not accepted and a uniform duct exit flow is desired to obtain an efficient IPT/LPT.

The lack of experimental data for turbine ducts, initiated studies in several EU-programs (AIDA, AITEB2 and DREAM). At Chalmers, a new LSLS turbine facility was built and different duct configurations were studied, see Arroyo [1], Arroyo et al. [2], Axelsson [3] and Axelsson et al. [4]. The duct configuration studied by Arroyo, included a non-turning structural vane, and flow and heat transfer was measured. Comparison to CFD predictions of these flows have been presented in Wallin [5]. Additional investigations of turbine ducts have been performed at Graz University, Marn et al. [6] and [7] and Göttlich et al. [8], [9] and [10], where a transonic turbine facility has been used. Flow and heat transfer investigations for an IP vane configuration has been presented in Povey et al. [11]. However, there is still a need of additional insight of the flow and heat transfer of turbine ducts, and the use of an LSLS facility allows detailed measurements to be conducted in order to fill this gap.

The main objective of this investigation is to study the flow characteristics of a turbine duct with a low turning vane, in order to provide a well-defined test case for CFD validation. This paper presents the new turbine duct configuration and initial measurements in comparison to CFD prediction.

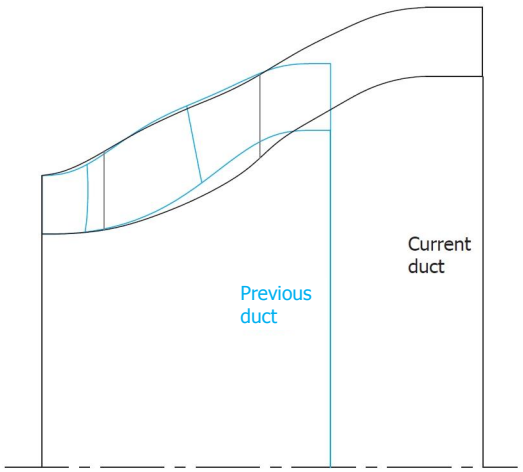

FIGURE 1. COMPARISON OF THE NEW AND THE PREVIOUS DUCT, ARROYO ET AL. [2].

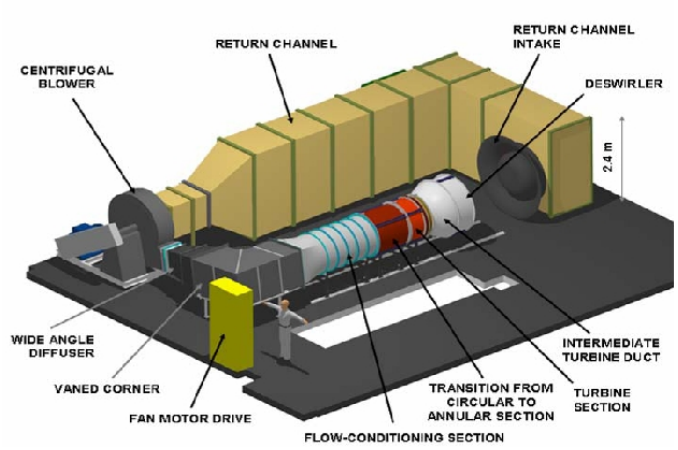

FIGURE 2. CHALMERS LSLS TURBINE FACILITY.

NOMENCLATURE

C	Cord length of the guide vane
C_p	Pressure coefficient
C_{pt}	Total pressure coefficient
P	Static pressure
P_{ref}	Reference pressure outside rig
P_t	Total pressure
q_{in}	The dynamic pressure at inlet
U_x	Axial velocity
x	Coordinate in axial direction
α	Swirl angle
ω_x	Axial vorticity

ABBREVIATIONS

CFD	Computational fluid dynamics
HPT	High pressure turbine
IPT	Intermediate pressure turbine
LPT	Low pressure turbine
LSLS	Large-scale low-speed

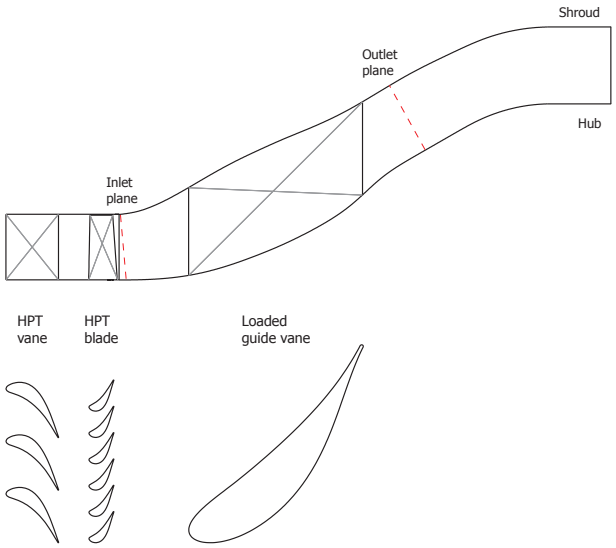

FIGURE 3. TURBINE DUCT SHOWING THE INLET AND OUTLET PLANES.

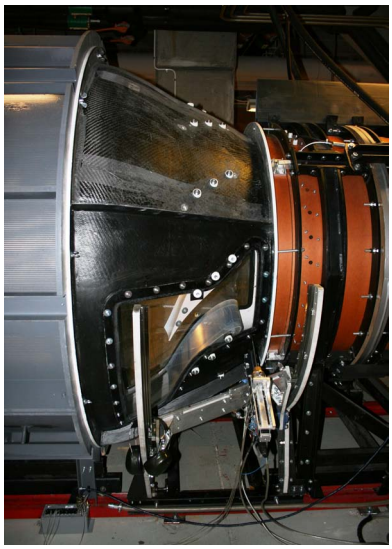

FIGURE 4. TEST SECTION OF THE EXPERIMENTAL FACILITY.

EXPERIMENTAL APPARATUS AND PROCEDURES

Chalmers Turbine Facility

To conduct the present investigation, the turbine facility at Chalmers University shown in Fig. 2 has been used. It is a large-scale low-speed closed loop facility powered by a centrifugal blower of 100 kW. The turbine disc/axis is controlled by a hydraulic brake to enable constant running conditions. The return flow runs through a cooling device enabling constant temperature before entering the centrifugal fan again. The HPT vanes and blades, corresponding to the second stage of a two-stage HPT, generate realistic inlet conditions to the duct. The inlet conditions, e.g. flow angles, can be varied by changing the relation between the axial flow velocity and turbine speed. However, limited by the maximum axial velocity of 30 m/s and turbine speed of 1300 rpm. A more detailed description of the facility, though with another turbine duct, can be found in Arroyo [1], Arroyo et al. [2], Axelsson [3] and Axelsson et al. [4].

Test Section

For this experimental investigation, a new turbine duct and guide vanes have been designed. The design work for the new configuration has been performed using Volvo Aero design tools (VolVane) and CFD analysis. The limitations and aims of the design were given by:

- The existing rig at Chalmers, i.e. the geometry at the inlet (hub and shroud radius), flow angles, mass flow.
- The duct and vane should be of a typical and modern design with robustness to varying inlet conditions, and to give a non-separated flow with low losses.

The new configuration is shown in Fig. 3 and a comparison with the previous duct in Fig. 1. The duct was also fitted with windows on both hub and shroud to enable optical access during the measurements, seen in Fig. 4.

Measurement Procedure

The flow field has been measured by multi-hole pressure probes. A seven-hole probe was used to study the flow in the two measurement planes defined in Fig. 3. The probe is an L-type probe with a head diameter of 2 mm, individual distances between the holes of 0.5 mm and a tip half-cone angle of 30 degrees. It was calibrated at a velocity of 25 m/s and for flow angles between 0 and 72 degrees. A three-axis traversing system has been used to position the probe in the test section. The positioning is controlled by stepper motors with a resolution of better than 5 μm and 0.001 degrees. The initial positioning of the pressure probe is estimated by the authors to have a tolerance of $\pm$0.1 mm in the radial coordinate and $\pm$0.2 degrees in swirl angle.

The pressures were sampled using a 16-channel PSI 9116 digital pressure scanner (Pressure Systems Inc.) with a measuring range of $\pm$2500 Pa. The probe measurements were carried out in positions according to a mesh that covers a two dimensional area between two consecutive vanes, i.e. 30 degrees, and with a denser distribution close to the hub and shroud to capture

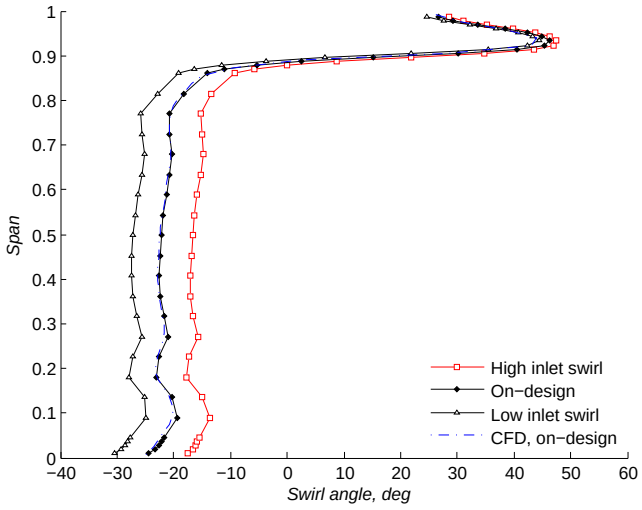

FIGURE 5. MASS AVERAGED SWIRL ANGLE PROFILE AT INLET.

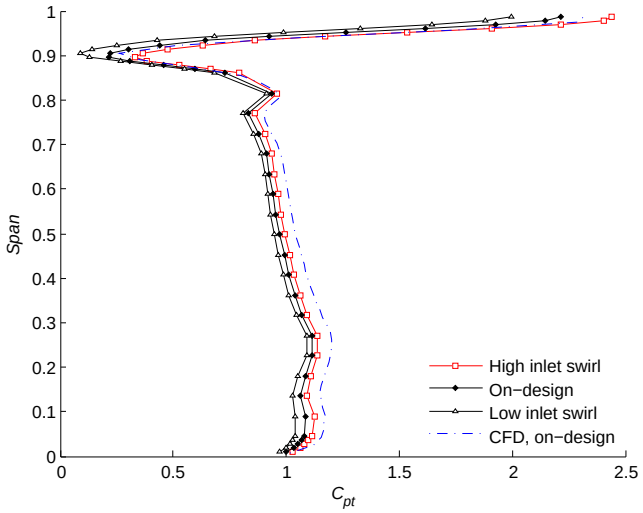

FIGURE 6. MASS AVERAGED TOTAL PRESSURE COEFFICIENT PROFILE AT INLET.

the influence from the tip leakage flow.

To measure the static pressure on the guide vane itself, it has been fitted with a high number of pressure taps. The distribution of these taps is denser in critical regions, such as the leading and trailing edges and close to the hub and shroud. The pressure taps were scanned using a Scanivalve mechanical multiplexer connected to the same PSI 9116 system used for the probe measurements.

The mean pressures were evaluated from the averaging of over 1000 samples acquired at 500 Hz sampling rate.

Some of the measurements has been repeated, with identical results, which confirm sampling times and accuracy.

Operational Conditions

By altering the load from the hydraulic brake on the turbine, the turbine speed changes, giving different operating conditions. In this study three different operating conditions have been investigated, an on-design condition (inlet swirl angle of around -22 degrees at mid span) and a high swirl and low swirl condition, see Fig. 5. Higher load on the turbine gives a lower aerodynamic load on the guide vane i.e. lower inlet swirl angle, the corresponding case in this study is the -27 degrees conditions. The case with lower load on the turbine corresponds to a -17 degrees inlet swirl angle into the duct.

NUMERICAL SETUP

The CFD analysis have been performed using ANSYS-CFX (v12.1), with a $k-\Omega$ SST turbulence model. The mesh used is of order 2.2 million cells, with resolved boundary layers, and results

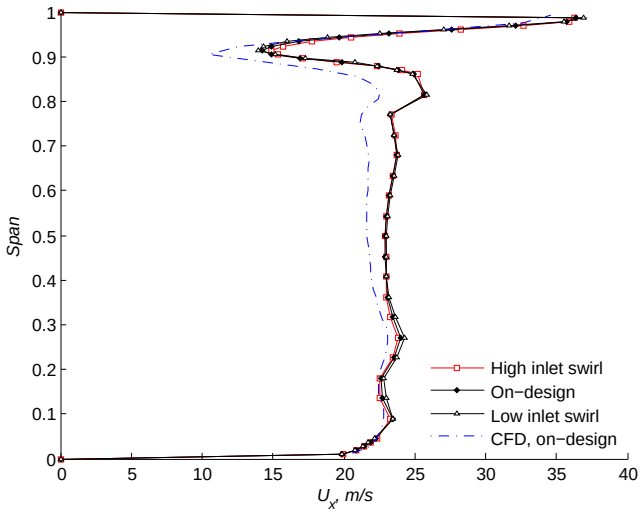

FIGURE 7. AVERAGED AXIAL VELOCITY PROFILE AT INLET.

have been checked to be mesh-independent. The measured 1D radial profiles, based on the inlet plane measurements, of the total pressure and swirl angles, see Fig. 5 and 6, was used as inlet conditions, together with a massflow. CFD analysis is performed for the on-design case only.

RESULTS AND DISCUSSION

The measurements presented from the pressure probe at the inlet and outlet planes, are all averaged over 30 consecutive degrees, spanning the distance between two guide vanes.

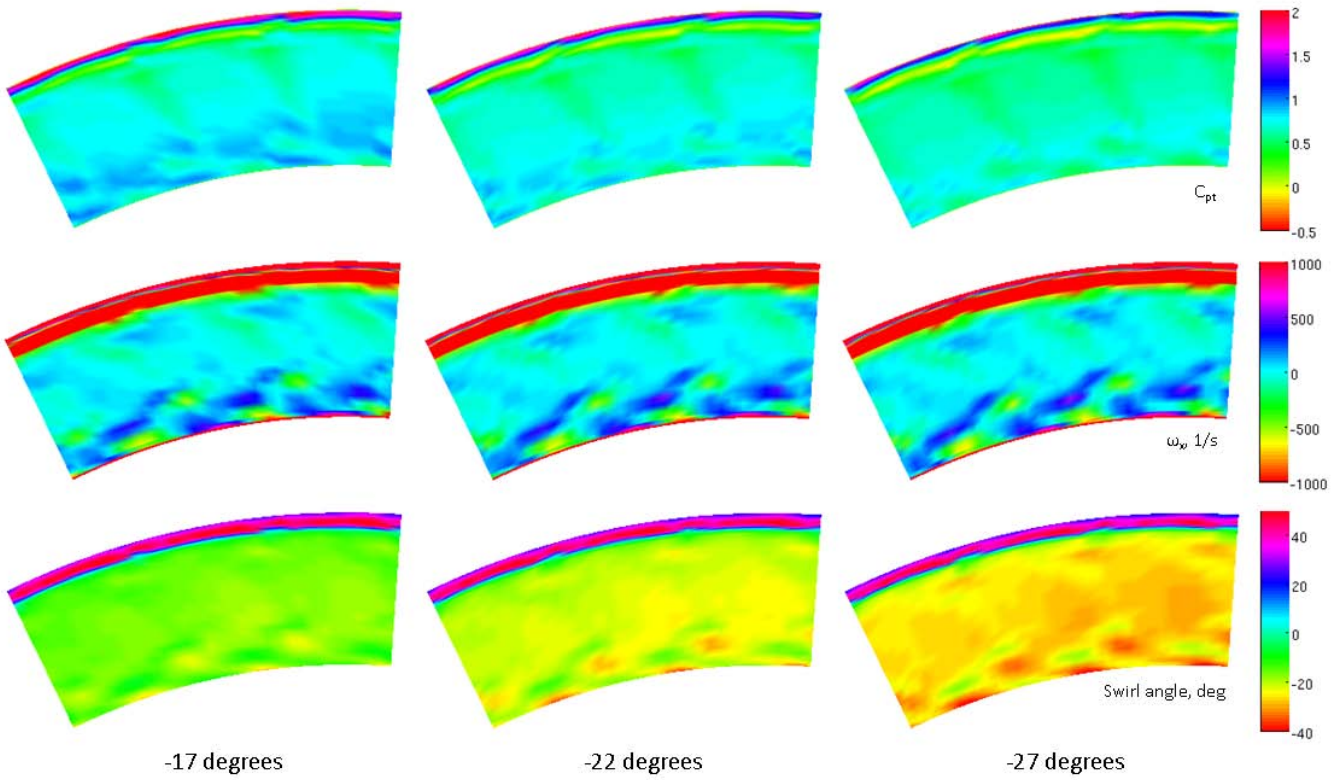

FIGURE 8. EXPERIMENTAL INLET CONTOURS OF THE PRESSURE COEFFICIENT, VORTICITY AND SWIRL ANGLE.

The static pressure coefficient is given by Equation. 1. By exchanging the static pressure with the total pressure in Equation. 1 the total pressure coefficient is also given.

$$C_p = \frac{P - P_{ref}}{q_{in}} \tag{1}$$

Inlet Conditions

Fig. 5 shows the averaged radial profile of swirl angle at the inlet plane for the three operating conditions. As noticed, the swirl angle at mid span differs between the on-design (-22 degrees) and off-design (-17 and -27 degrees), cases. The tip leakage between the HPT blade tip and the shroud is clearly seen as the rapid change in swirl angle closer to the shroud.

The influence of the tip leakage is also clearly seen in the total pressure coefficient and axial velocity magnitude, see Fig. 6-7. As noticed from Fig. 5-7, the effect of the tip leakage covers a significant region close to the shroud, which could be connected to the presently used large tip gap, of order 1.5% of the blade span.

Contours of the total pressure coefficient, axial vorticity and swirl angle in the measurement plane for the three operating conditions studied are plotted in Fig. 8. The duct inlet measurements clearly show a non-uniform inlet flow, with traces from upstream HPT vanes. This flow pattern has also been presented in Arroyo [1], and it is connected to the vortex structures in upstream HP vane which passes through the rotating blade into the duct. The flow pattern for the different operating conditions is similar.

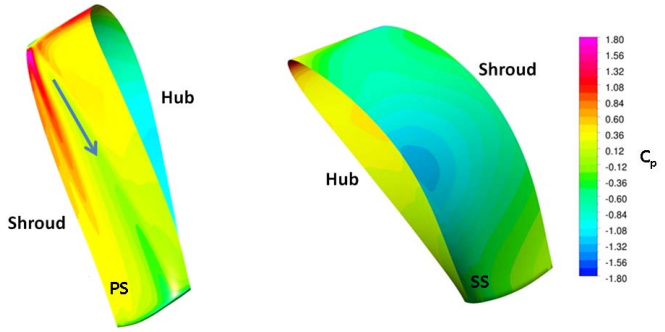

FIGURE 10. STATIC PRESSURE COEFFICIENT FOR THE PRESSURE AND SUCTION SIDE OF THE GUIDE VANE FROM THE CFD PREDICTIONS.

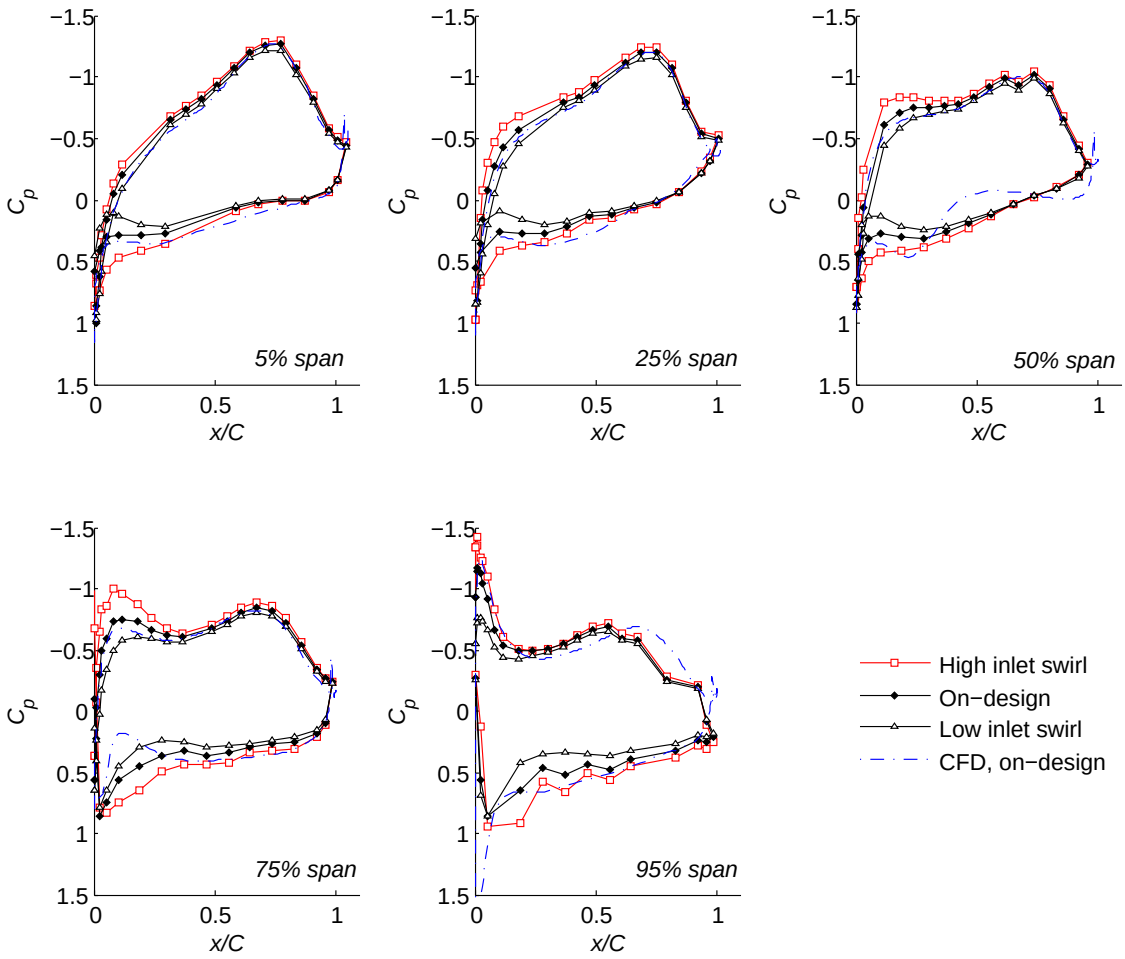

FIGURE 9. STATIC PRESSURE COEFFICIENT FOR THE FIVE SPANS ON THE GUIDE VANE.

Static Pressure on the Vane

In Fig. 9 the static pressure coefficient is plotted for the five different spans on the guide vane where the pressure taps were located. The leading edge of the guide vane is located at $x/C = 0$ and the trailing edge is at $x/C = 1$. The variation of the pressure coefficient around the leading edge for the three operating conditions is explained by the different inlet incidence angles. The "*high inlet swirl*" case (inlet swirl of -17 degrees at mid span) require more turning than the other cases, and thus a higher pressure difference between pressure and suction side at the front part of the vane. The figure also includes CFD results for the on-design case, and a fairly good agreement is observed. In the results closest to the shroud, 95% *span*, there is a slight difference between experiments and CFD on the suction side close to the trailing edge. This is most probably explained by small apparent irregularities in this area of the shroud window in the experimental setup.

The fact that the results from all three operating condition in experiments and the simulations coincide from about $x/C = 0.6$, except for the 95% *span*, shows that the guide vane is turning the flow according to what is desired and indicates that the flow around the vane is not separated.

The CFD results of the static pressure coefficient on the vane is presented in Fig. 10, and this explain some of the deviation between CFD and measurements observed in Fig. 9. At the pressure side of the vane, a low pressure streak is observed in the CFD analysis. This streak is explained by a vortex caused by the tip leakage flow, as shown in Fig. 11 and 12. However, the measurements does not give evidence of this low pressure streak, which could be explained by the limited resolution of pressure taps in the measurements, or the inlet conditions used by the CFD in the tip leakage region.

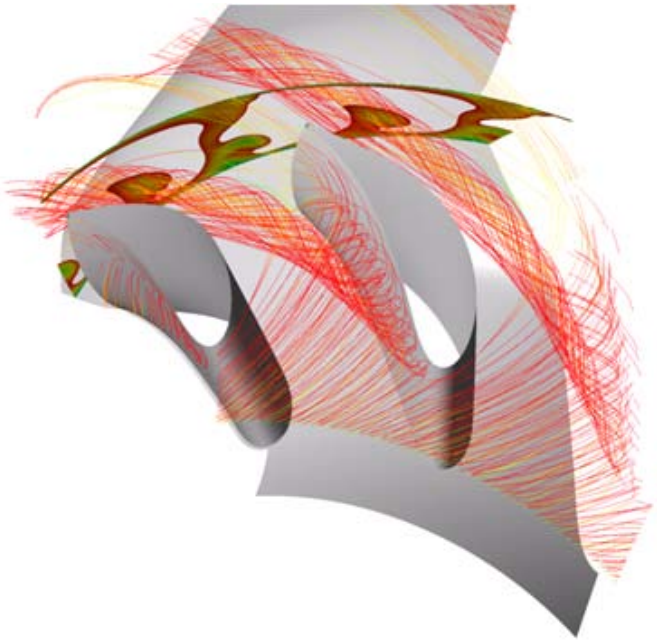

FIGURE 11. PATHLINES RELEASED AT THE TIP REGION, ABOVE 90%, SPAN AND TRACED BACKWARDS FROM THE LOW TOTAL PRESSURE COEFFICIENT ON THE OUTLET PLANE.

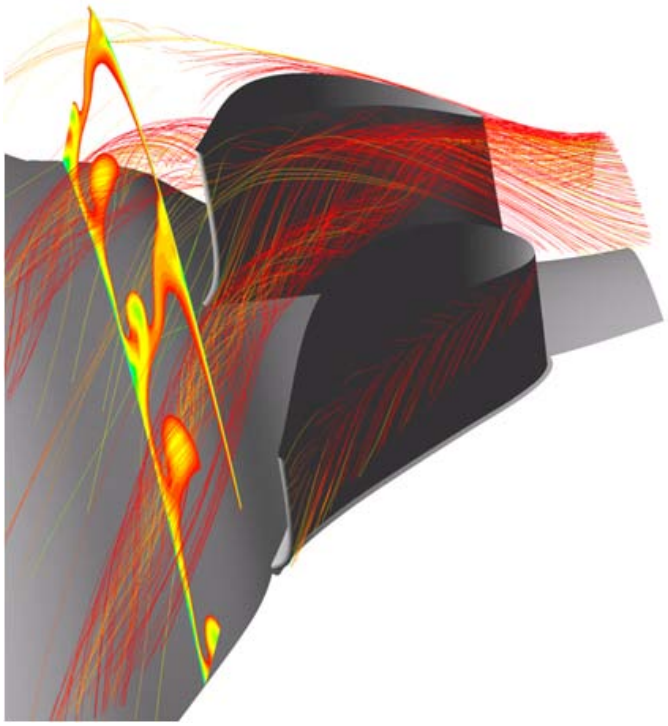

FIGURE 12. PATHLINES RELEASED AT THE TIP REGION, ABOVE 90%, SPAN AND TRACED BACKWARDS FROM THE LOW TOTAL PRESSURE COEFFICIENT ON THE OUTLET PLANE.

Outlet Conditions

The pressure probe measurements were also carried out just behind the vane, see Fig. 3. The position of the outlet plane is chosen due to physical limitations of the traverse system used for the measurements. It is also evident that possible separations and pressure losses behind the guide vane are more easily detected closer behind the vane than at the actual outlet plane of the duct.

Fig. 13 shows contours of the measured total pressure coefficient at the outlet plane for the three different operating conditions. The contours shown in the figure is for a 60 degree sector, i.e. for two vane passages. The total pressure field at the outlet looks similar for the different operating conditions and indicates the largest loss region close to the hub, which is mainly explained by the vane-hub corner vortex. Similar, but weaker, loss region is found close to the shroud and it is also noticed that the wake is quite weak in the measurements.

CFD results, for the on-design case, are shown in Fig. 14, which indicate a slightly different outlet total pressure field compared to the measurements. The CFD results predicts an additional loss region in the middle of the sector, slightly away from the hub, and the wake is more evident. The additional loss region is connected to the vortex created by the tip leakage flow, as shown in Fig. 11 and 12. It has in previous studies been shown that this vortex travels from the shroud towards the hub due to the static pressure gradient pushing it, see for example Marn [7], which is supported by the visualization in Fig. 11 and 12 and also mentioned when discussing the CFD results in Fig. 9-10.

Thus, the difference in outlet total pressure fields between the measurements and CFD results might be connected to the tip leakage flow at the inlet. The pressure probe measurements in the tip leakage region at the inlet plane is subject to larger uncertainty due to large gradients in the flow. Sensitivity studies of the CFD inlet condition in the tip leakage region shows influence on the predicted vortex structure and the outlet plane total pressure loss regions. Another possible explanation for the difference between the CFD and measurement results might be that the current CFD results are steady state analysis using 1D radial profiles at the inlet, whereas the real flow in the rig is unsteady with non-uniform structures at the inlet plane, seen in Fig. 8, which is expected to increase the mixing.

Note that the contour scale in Fig. 13 and 14 is slightly different, which is due to difference in average pressure loss. CFD predictions indicate around 30% higher losses compared to the measurements.

The radial profiles at the outlet plane is found in Fig. 15-17, showing the swirl angle, total pressure coefficient and axial

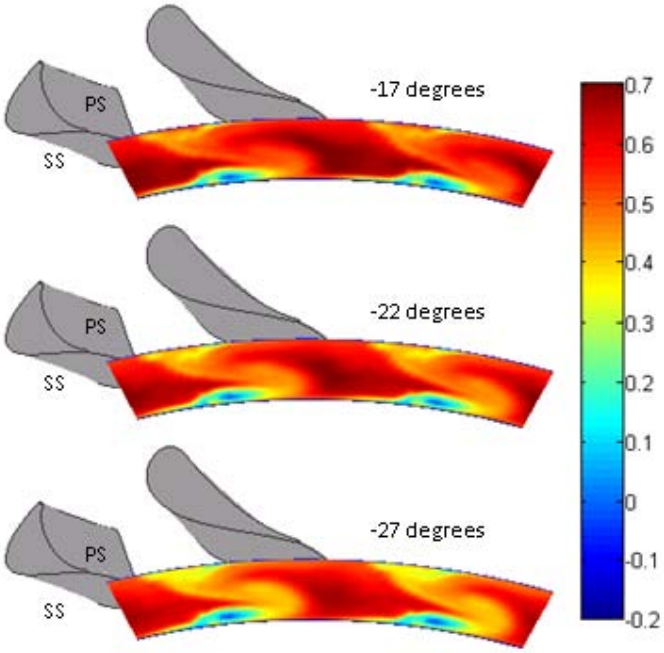

FIGURE 13. OUTLET CONTOUR OF THE TOTAL PRESSURE COEFFICIENT, FROM EXPERIMENTS.

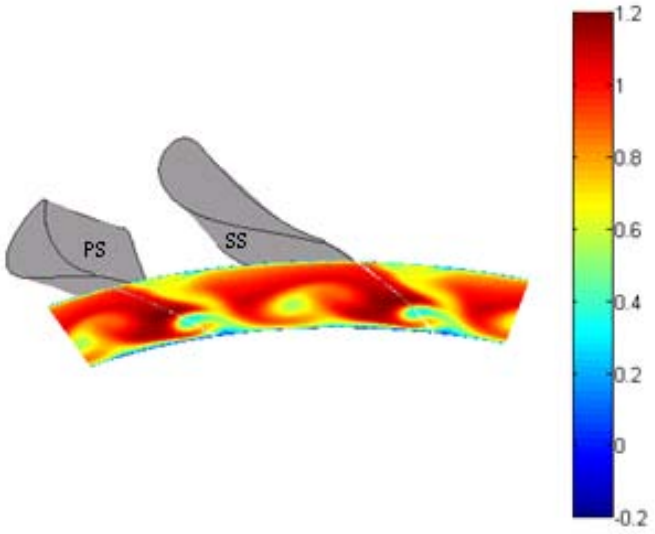

FIGURE 14. OUTLET CONTOUR OF THE TOTAL PRESSURE COEFFICIENT, FROM CFD PREDICTIONS.

velocity. The measurements at different operating conditions is shown in comparison to CFD results for the on-design case. The measured profiles for different operating conditions show a similar shape, which indicates that the duct exit condition is fairly robust to changes in the inlet swirl and that the vane is doing a good job. A comparison of CFD and measurements, indicate that the turning of the flow is good in average, but the radial distribution is slightly different. The differences between CFD and measurement results might be explained by the vortices and secondary flows, as discussed above. The CFD analysis indicate a slightly lower axial velocity, which might be connected to a used lower mass flow.

CONCLUSIONS

A new design of both the duct and its vanes has been developed, built and installed into the already existing large-scale low-speed turbine facility at Chalmers University. Experiments have been conducted on this new setup, studying the aerodynamic performance of the design in the purpose of producing good quality validation data for CFD models. This has been achieved and presented in this paper together with a comparison with the corresponding CFD simulations. The measurements include an inlet plane describing the flow into the duct, the static pressure acting on the guide vanes and an outlet plane measurement at three different operating conditions.

In conclusion, the new design of the duct and vane has good performance and is robust to changed inlet swirl. The most significant loss at the outlet is found close to the hub and is believed to be connected to the suction side corner vortex. The agreement between CFD and measurements is observed to be fairly good. Some differences are found in the static pressure on the pressure side of the vane, and in the total pressure field at the outlet. This is believed to be connected to the predicted vortex structure, originating from the tip leakage.

From varying swirl angles and pressure distributions within this region in the inlet conditions to the CFD simulations it is seen that the flow develops in different ways inside the duct. The intensity of the passage vortex is strongly influenced by these variations which also gives that the pressure losses are effected. Hence, the importance of modelling this region in a correct way is crucial in order to achieve valid results.

ACKNOWLEDGMENTS

The work within this project was carried out with financial support from the Swedish National Aeronautics Research Programme (NFFP), which is acknowledged.

REFERENCES

[1] Arroyo Osso, C., 2009. “Aerothermal Investigation of an Intermediate Turbine Duct”. PhD Thesis, Chalmers University of Technology, Göteborg, Sweden.

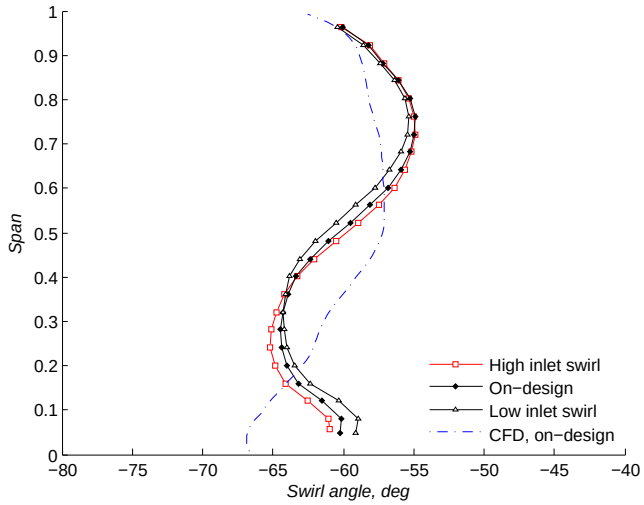

FIGURE 15. SWIRL ANGLE AT OUTLET.

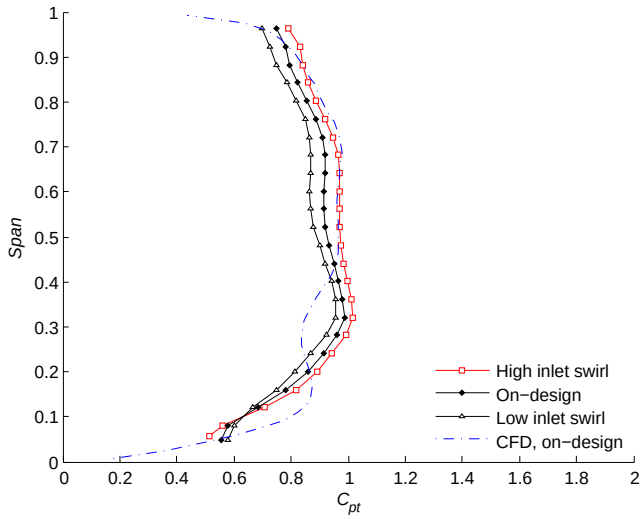

FIGURE 16. TOTAL PRESSURE COEFFICIENT PROFILE AT OUTLET.

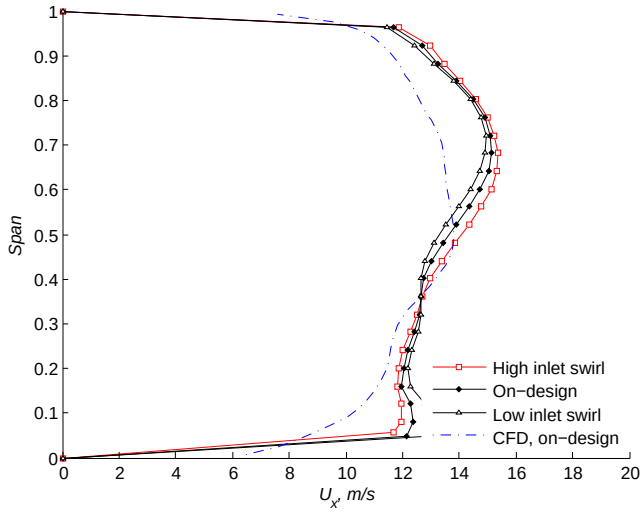

FIGURE 17. AXIAL VELOCITY PROFILE AT OUTLET.

[2] Arroyo Osso, C., Axelsson, L., Håll, U., Johansson, T. G., Larsson, J., and Hasselbach, F., 2006. "Large-scale low-speed facility for investigating intermediate turbine duct flows". In 44th AIAA Aerospace Sciences Meeting and Exhibit. AIAA-2006-1312.

[3] Axelsson, L.-U., 2009. "Experimental Investigation of the Flow Field in an Aggressive Intermediate Turbine Duct". PhD Thesis, Chalmers University of Technology, Göteborg, Sweden.

[4] Axelsson, L., Arroyo Osso, C., Cadrecha, D., and Johansson, T. G., 2007. "Design, Performance Evaluation and Endwall Flow Structure Investigation of an S-shaped Intermediate Turbine Duct". In ASME Turbo Expo 2007. GT2007-27650.

[5] Wallin, F., 2008. "Flow Control and Shape Optimization of Intermediate Turbine Ducts for Turbofan Engines". PhD Thesis, Chalmers University of Technology, Göteborg, Sweden.

[6] Marn, A., Göttlich, E., Pecnik, R., Malzacher, F. J., Schennach, O., and Pirker, H. P., 2007. "The Influence of Blade Tip Gap Variation on the Flow Through an Aggressive S-shaped Intermediate Turbine Duct Downstream a Transonic Turbine Stage - part I: Time-averaged Results". In ASME Turbo Expo 2007. GT2007-27405.

[7] Marn, A., Göttlich, E., Cadrecha, D., and Pirker, H. P., 2006. "Shorten the Intermediate Turbine Duct Length by Applying an Integrated Concept". In ASME Turbo Expo 2008. GT2008-50269.

[8] Göttlich, E., Woisetschläger, J., Pieringer, P., Hampel, B., and Heitmeir, F., 2006. "Investigation of Vortex Shedding and Wake-Wake Interaction in a Transonic Turbine Stage Using Laser-Doppler-Velocimetry and Particle-Image-Velocimetry". *Journal of Turbomachinery,* ***128***, pp. 178–187.

[9] Göttlich, E., Marn, A., Pecnik, R., Malzacher, F. J., Schennach, O., and Pirker, H. P., 2007. "The Influence of Blade Tip Gap Variation on the Flow Through an Aggressive S-shaped Intermediate Turbine Duct Downstream a Transonic Turbine Stage - part II: Time-resolved Results and Surface Flow". In ASME Turbo Expo 2007. GT2007-28069.

[10] Göttlich, E., Marn, A., Malzacher, F. J., and Heitmeir, F., 2009. "On Flow Separation in a Super-Aggressive Inter-

mediate Turbine Duct". In 8th European Conference on Turbomachinery Fluid Dynamics and Thermodynamics.

[11] Povey, T., Chana, K. S., and Jones, T. V., 2003. "Heat Transfer Measurements on an Intermediate-Pressure Nozzle Guide Vane Tested in a Rotating Annular Turbine Facility, and the Modifying Effects of a Non-Uniform Inlet Temperature Profile". *Proc Instn Mech Engrs Part A: Journal of Power and Energy,* ***217***, pp. 421–431.